Analyzing Collimator Rotation Angle Influence on Half-beam VMAT Outcomes for Prostate Cancer: A Comparative Approach Using Statistical and Machine Learning Methods

Myeongsoo Kim

Keimyung University Dongsan Hospital

Byungyong Kim

Keimyung University Dongsan Hospital

Euncheol Choi

Keimyung University Dongsan Hospital

Yun Sung Shin

Keimyung University Dongsan Hospital

Seung Gyu Park

Keimyung University Dongsan Hospital

Young Kee Oh

Keimyung University Dongsan Hospital

Sang Jun Byun

kryph@dsmc.or.kr

Keimyung University Dongsan Hospital

Additional Declarations: No competing interests reported.

Abstract

Purpose

This study explores the impact of Collimator Rotation Angle (CRA) settings in Half beam Volume Modulated Arc Therapy (HVMAT) for prostate cancer treatment, focusing on dose distribution and treatment efficacy.

Materials and Methods

Treatment plans (Total 240) for 20 prostate cancer patients were developed using HVMAT. Different CRA settings (n = 12) were employed, specifically comparing 2-arcs and 4-arcs techniques. Data were analyzed using statistical methods and machine learning models, assessing the Mean Relative Error (MRE) across varying CRA settings.

Results

The analysis revealed no significant impact of CRA settings on the conformity and homogeneity of radiation distribution to the target volume. All treatment plans met the average V95% target for the prescribed dose in the Planning Target Volume (PTV). Machine learning analysis showed consistent predictive accuracy across different CRA settings, with the MRE variance within 2%. Statistical tests further supported these findings, showing no significant differences in treatment plan outcomes based on CRA variations.

Conclusion

The study demonstrates that CRA settings in HVMAT can be selected with considerable flexibility without compromising the effectiveness of prostate cancer treatment. The results emphasize the importance of employing multi-faceted analysis, including both traditional statistical methods and advanced machine learning techniques, in optimizing HVMAT treatment plans. Although limited by a small sample size and a specific focus on prostate cancer, the findings provide valuable insights into the clinical application of HVMAT and its potential in treatment plan optimization.

1. INTRODUCTION

Volume-modulated arc therapy (VMAT) is an advanced radiation therapy technique that delivers high doses (cGy) to tumors while limiting exposure to normal organs. The use of arc beams in VMAT simplifies planning by reducing variability in beam directions. However, a downside of VMAT is the increased dose intensity in low-dose regions due to beam segmentation by rotation angles [1].

Several methods have been proposed for beam delivery optimization in VMAT, focusing on dose optimization algorithms and beam delivery techniques [2]. Studies have explored advanced VMAT dose optimization algorithms, proposing the maintenance of beams at 2° intervals to enhance beam angle resolution [3].

In pelvic tumors such as cervical and prostate cancers, large Planning Target Volumes (PTVs) that include surrounding lymph nodes are common. As the volume of the PTV increases, VMAT techniques face physical limitations in the speed and distance of Multi-Leaf Collimator (MLC) movements. Particularly, PTVs, often concave in shape due to adjacent Organ at Risks (OARs) like the bladder and rectum, increase the complexity of MLC aperture design. Increased complexity in MLC can make it more challenging to deliver the planned treatment [4, 5, 6].

Multiple studies have investigated the impact of Collimator Rotation Angle (CRA) on optimal dose distribution in VMAT treatment plans [7–12]. Variations in dose delivery due to differences in CRA angles have been reported. In current VMAT, dynamic collimator rotation during beam delivery is not permitted, thus making it crucial to decide CRA for each arc before optimization [13]. Sun et al found that intersection angle of 2-arcs, $\Delta\theta$, significantly influence VMAT plans, with plan quality almost consistently improving as $\Delta\theta$ approaches 90° [11].

Recent studies in pelvic tumors have progressed with Half beam-VMAT (HVMAT) to reduce beam leakage and MLC movement associated with MLC. HVMAT is based on 2-arcs with the same CRA, each blocking half of the field from the central axis (CAX), optimizing MLC apertures for the opened areas [14–17]. Yu et al evaluated HVMAT for cervical cancer treatment with concave PTVs, showing better outcomes in terms of Conformity Index (CI), Homogeneity Index (HI), D2%, and V107% compared to VMAT. However, their study lacked data on CRA, limiting the evaluation of HVMAT treatment plans.

The approach in HVMAT differs from traditional VMAT methods. To apply the effects of varying collimator angles, HVMAT requires a higher number of arcs compared to VMAT. In such scenarios, not thoroughly assessing rotation angles before applying the HVMAT technique could lead to ambiguity in CRA settings. Therefore, it is essential to rigorously evaluate the choice and setting of rotation angles for the effective application of VMAT and HVMAT techniques. Particularly, this study overcomes the limitations of traditional statistical analysis and utilizes machine learning to deeply analyze the complex and nonlinear relationships between CRA and clinical variables. Through this approach, the study aims to gain a more precise understanding of how subtle variations in CRA can affect the quality of treatment planning and the accuracy of beam delivery.

2. MATERIALS AND METHODS

2.1 Plan preparation

In this study, HVMAT treatment plans were established for 20 patients with stage   to   a prostate cancer who were diagnosed with adenocarcinoma and received postoperative radiotherapy or single

radiotherapy.

The scan was performed in the full bladder condition to limit the dose to the small bowel. The bladder volume was prepared to be 180 cc–250 cc by drinking sufficient water 1 hour before the Computed Tomography (CT) scan for treatment planning and checking the bladder volume using an ultrasound scanner. A balloon catheter for radiotherapy was inserted into the rectum for dose sparing, and 60 cc of air was injected.

The treatment target and OAR structures were delineated on the treatment-planning CT images. The clinical target volume (CTV) was delineated according to the NRG Oncology and Radiation Therapy Oncology Group (RTOG) consensus guidelines [18]. The upper pelvic margin of the CTV began within the L5–S1 range. Moreover, the common iliac nodal, right and left internal and external iliac nodal, and obturator nodal regions were included. A 7 mm margin was expanded in the vessels around the nodal region. The PTV was created by extending 3 mm from the CTV in the posterior direction and 5 mm in the other direction.

2.2 HVMAT planning

FIGURE 1. Patient #5, Example of collimator rotation angle 15°/15°: Beam's eye view of half-beam volumetric modulated arc therapy including the half-beam fields corresponding to 2-arcs of gantry rotation: (a) counterclockwise (Gantry rotation angle: 179.0°–181.0°) and (b) clockwise (Gantry rotation angle: 181.0°–179.0°).

FIGURE 2. Patient #5, Example of collimator rotation angles 15°/0° and 15°/285°: Beam's eye view of half-beam volumetric modulated arc therapy, encompassing the half-beam fields corresponding to 4-arcs of gantry rotation: (a) 4-arcs with collimator rotation angle 15°/0°, and (b) 4-arcs with collimator rotation angle 15°/285°.

The prescribed dose of the PTV was 4500 cGy with 180 cGy per treatment. The treatment plan used Eclipse™ treatment planning system, version 15.5 (Varian Medical Systems, Palo Alto, CA, USA). The linear accelerator (LINAC) machine is a VitalBeam™. The integrated MLC comprised 60 opposing leaf pairs, with a 5 mm leaf in the isocenter area and a 10 mm leaf in the rest.

In this study, we focused solely on the effects of 15 MV photon beam intensity, excluding the varying opinions regarding treatment outcomes and OAR sparing. That is, the energy used in this study was set to 15 MV photon beam at a dose rate of 600 MU/min according to the treatment protocol of our institution. Dose-volume calculations were performed using the anisotropy analysis algorithm version 15.5.12. The 0.25 cm calculation resolution was applied.

Each HVMAT treatment plan is adjusted to form a Half field by shielding the right or left field with the CAX as the reference on the X-axis. Four treatment plans were created by changing the CRA to 15°/15°, 30°/30°, 45°/45°, and 60°/60° with 2-arcs. In each plane, there are two coplanar arcs: clockwise (CW) arc (181.0°-179.0°) and counterclockwise (CCW) arc (179.0°-180.0°).

Treatment plans were developed by adjusting the CRA at different orientations. Specifically, four plans with cross angles below 90° were established, with angles set at 15°/0°, 30°/0°, 45°/0°, and 60°/0° with 4-arcs. Additionally, another four plans with a precisely 90° cross angle were generated, featuring angles of 15°/285°, 30°/300°, 45°/315°, and 60°/330° with 4-arcs. This resulted in a total of 8 treatment plans, each incorporating four coplanar arcs corresponding to the CRA.

The configuration of the two collimator angles is denoted as θ_1/θ_2, representing the angles of the first and second arcs. The intersection angle between these two angles, identified as $\Delta\theta$, ranged from 0° to 90°.

2.3 Planning optimization

A template was created to proceed with dose optimization by assigning the same dose-volume histogram (DVH) constraint weight to 12 plans of HVMAT, and an automatic normal tissue objective function was applied.

A jaw tracking function was not used, and the automatic optimization mode and intermediate dose were applied. The PTV set the priority weight to 400. The critical OARs were set as 200 to bladder, 150 to rectum, and 200 to small bowel, and the weight of the ring structure to 200. Using the PTV structure, the outer wall margin was extended by 0.3 cm, and the inner wall margin was extended by 0.3 cm to the inside to create a ring structure.

The dose and priority values did not change during the optimization, and each multi-resolution level was automatically processed without interference. In the case of PTV, more than the prescribed dose satisfied D95% of the PTV.

2.4 Evaluation metrics

Conformation number (CN) and HI were analyzed to evaluate the changes in dose distribution for CRA differences in the HVMAT treatment plan [19, 20].

The CN was proposed by van't Riet et al., and the formula is as follows [21]:

$$CN = (TVRI)\,2/\,(TV * VRRI)$$

1

……………………………………………………………………………..

where TV_{RI} is the target volume covered by the reference isodose, TV is the target volume, and V_{RI} is the volume of the reference isodose indicating the "95% isodose of prescribed dose."

HI is presented in RTOG as follows.

$$HI = (D2\%/D98\%)/prescribed\,dose$$

……………………………………………………………………………………..

D2% is defined as the minimum dose in 2% of the target, indicating the "maximum dose," and D98% is defined as the minimum dose in 98% of the target, indicating the "minimum dose."

We aimed to assess the impact of CRA on the radiation dose distribution delivered to normal organs. To achieve this, we quantitatively evaluated the risk of treatment-related toxicity. For this purpose, we calculated the normal tissue complication probability (NTCP) based on the analysis of radiation dose distribution in healthy organs.

The Lyman-Kutcher-Burman (LKB) NTCP model quantitatively evaluates the impact of both the radiation dose and the volume of the gland irradiated on the likelihood of radiation-induced changes. The TD_{50} represents the dose for uniform irradiation of the entire or partial volume resulting in a 50% probability of a complication. The equivalent uniform dose (EUD) concept has also been utilized in normal tissues to assess the harm of a non-uniform dose distribution with the same outcome as a specific uniform dose.

The formula for NTCP is as follows:

$$NTCP = \frac{1}{\sqrt{2\pi}} \int_{-\infty}^{t} e^{-\frac{x^2}{2}} \, dx$$

$$t = \frac{EUD - TD_{50}}{m \cdot TD_{50}}$$

$$EUD = \left(\sum_{i=1}^{N} v_i D_i^{1/n} \right)^n$$

………………………………………………………………………………….(3)

In this context, N represents the organ's voxel count. The D_i denoting the dose assigned to the i-th voxel and v_i indicating the volume of the i-th voxel. The parameter n serves to characterize the biological attributes of the organ [22].

Modulation Complexity Score (MCS) was modified by Masi et al. from original quotation [23].

$$MCS = \sum_{i=1}^{S-1} \left(\frac{AAV_i + AAV_{i+1}}{2} \times \frac{LSV_i + LSV_{i+1}}{2} \times \frac{MU_{i,i+1}}{MU_{beam}} \right)$$

………………………………………………………………………………….(4)

The MCS was analyzed to compare and evaluate the complexity of the HVAMT treatment plans. McNiven et al. introduced the MCS, which is determined by combining two factors: leaf sequence variability (LSV) and aperture area variability (AAV). LSV assesses field irregularity by comparing adjacent leaf positions,

while AAV evaluates the variation in field area from a maximum area. The MCS is conceptualized as a straightforward score ranging from 0 to 1, where a score of 1 indicates a plan without modulation.

Lam et al. developed an in-house program with a Python package and calculated the aforementioned metrics using the data extracted from the plan file [24]. We analyzed MCS using the Python package provided by Lam et al. As the complexity of the plan increased, the difference in the accuracy of the delivered beam increased. 5 patient plans were selected based on PTV size to confirm the beam delivery accuracy of the generated plans.

Patient quality assurance (QA) was performed to evaluate the Gamma Index (γ- index, 3 mm/3%) in different axes (local, global, and volumetric) using an electronic portal imaging device attached to a LINAC.

2.5 Data evaluation: Statistics and Machine learning

In this study, we calculated Pearson correlation coefficients using Python to quantify the relationships between clinical variables. These coefficients, ranging from − 1 to 1, represent the degree of correlation between pairs of variables. The relationships were visualized as heatmaps using seaborn and matplotlib libraries.

Following this initial analysis, we delved deeper into the complex and sometimes nonlinear relationships within radiation therapy planning. To address the complexity of the data, we employed the Random Forest model [25]. This machine learning model, consisting of an ensemble of decision trees, is effective in reducing variability and preventing overfitting. The Random Forest model also offers insights into the importance of features within the data.

For model construction, data specific to collimator rotation angles were extracted from the radiation therapy planning dataset, followed by necessary preprocessing. Separate models were then built and trained for each CRA setting. The performance of these models was evaluated using Mean Relative Error (MRE). MRE measures the average magnitude of relative errors between the predicted and actual values:

$$MRE = (1/n) * \sum (i = 1 to n) |(Yi - \hat{Y}i)/Yi|$$

……………………………………………………………………….(5)

Here, Yi represents the actual value, and Ŷi is the predicted value by the model.

Referencing the methodology of Smith et al., we compared Mean Relative Error (MRE) values across different Collimator Rotation Angle (CRA) settings. This comparison aided in assessing the impact of specific CRA settings on the outcomes of therapy plans. By following Smith et al.'s integrated approach of machine learning and statistical analysis, our aim was to enhance the reliability of our findings and to gain a better understanding of how different CRA settings influence the effectiveness of radiation therapy plans. Such an approach emphasizes the importance of multi-faceted analysis in the optimization of

radiation therapy, aligning with current trends in radiation therapy research [26]. Using this model, we analyzed how different settings of CRAs affect the outcomes of radiation therapy plans.

3. RESULTS

Table 1 presents the characteristics of patients and volumes for the target areas and OARs. The age range of the participating patients was between 47 and 85 years, with an average age of 71.7 years. All patients were diagnosed with adenocarcinoma. According to the TNM classification, 20 patients were in the range of T2aN0M0 to T4aN0M0, 2 were between T2a and T2c, 15 were between T3a and T3b, and 3 were diagnosed with T4a. 9 patients underwent both radiotherapy and surgery, while 11 patients received radiotherapy alone. The PTV ranged from 575 cm³ to 912.6 cm³ with an average of 753.9 cm³, the bladder volume varied from 150.4 cm³ to 441.7 cm³ with an average of 290.3 cm³, and the rectum volume was between 105.4 cm³ and 185.8 cm³, averaging 134.0 cm³. Specific data regarding the small bowel was not provided.

Table 1. Characteristics of patients and volumes for the target and OARs.

In this investigation, individualized treatment plans were developed for each of the 20 patients, incorporating diverse CRAs. Subsequently, the resulting CN and HI underwent a thorough multivariate analysis.

The statistical assessment, utilizing t-test, aimed to detect any noteworthy variations in treatment outcomes associated with different CRAs. However, the obtained p-values for the multivariate tests exceeded the significance threshold of 0.05.

This suggests that the selected CRAs did not induce statistically significant differences in CN and HI within the patient cohort. Upon scrutinizing the mean values and standard deviations provided in Table 2, it is evident that, notwithstanding the diversity in CRAs, the overall conformity and homogeneity of the dose distribution in the PTV were not significantly impacted by the chosen rotation angles.

These findings suggest that, within the confines of this study, adjustments to the CRA did not yield substantial variations in the conformity and homogeneity of the administered radiation dose to the target volume.

Consequently, the selection of CRA may not emerge as a pivotal factor influencing treatment efficacy in terms of PTV dose distribution for the examined patient population.

Table 2. Evaluation of PTV and OARs dose delivery (Mean ± SD, $n = 20$).

Table 2 presents an evaluation of dose delivery to PTV and OARs under different CRAs in 2-arcs and 4-arcs configurations. In terms of CN, the 2-arcs setup shows values ranging between 0.77 and 0.78, while the 4-arcs setup maintains a more consistent level around 0.80 in most cases. This suggests that the 4-

arcs setup may have slightly better radiation conformity to the target volume compared to the 2-arcs setup, although the difference is not substantially significant.

Regarding the HI, both the 2-arcs and 4-arcs setups maintain similar ranges, predominantly between 0.08 and 0.09. This indicates that both configurations achieve a comparable level of dose uniformity within the PTV.

In the context of total-NTCP (t-NTCP), the 2-arcs setup generally varies from 24.4 to 26.3, whereas the 4-arcs setup exhibits values between 24.2 and 26.0. These figures demonstrate that there is no significant difference in overall treatment toxicity between the two configurations. Additionally, within the 4-arcs setting, there is little variation in t-NTCP values between configurations with $\Delta\theta < 90°$ and $\Delta\theta = 90°$.

Overall, while the 4-arcs setup shows a slight advantage in radiation conformity to the PTV over the 2-arcs setup, both configurations offer stable treatment toxicity profiles, as evidenced by their t-NTCP values, without significant differences between them.

Table 3. Evaluation of machine performances (Mean ± SD, n = 20).

Table 3 presents an analysis of machine performance parameters, including Monitor Units (MUs), MCS, and Gamma Index, across various CRAs in both 2-arcs and 4-arcs configurations. In terms of MUs, the 2-arcs setup shows a slight variation across different angles, ranging from 1190.1 to 1226.7. In contrast, the 4-arcs setup demonstrates a broader range, with a notably higher MU value of 1337.4 at the 45°/315° CRA. This indicates increased beam complexity or intensity in the 4-arcs setting, especially at specific angles.

Regarding MCS, the values fluctuate across different angles for both configurations. However, there is no clear trend indicating a significant difference between the 2-arcs and 4-arcs setups in terms of complexity. The MCS values generally remain within a narrow range, suggesting a comparable level of complexity across the different settings.

The γ-index, a measure of treatment accuracy, varies slightly across different CRAs. In the 2-arcs configuration, the Gamma Index remains relatively high and consistent, indicating good treatment accuracy. The 4-arcs setup, particularly at $\Delta\theta = 90°$ angles (such as 45°/315°), shows a lower Gamma Index, suggesting a potential decrease in accuracy at specific angles.

Overall, the results in Table 3 illustrate that while there is some variation in machine performance parameters across different CRAs and configurations, the differences are not markedly substantial. However, specific angles in the 4-arcs setup, particularly at $\Delta\theta = 90°$, may present challenges in terms of increased beam complexity and slightly reduced accuracy, as indicated by higher MUs and lower γ index values.

Figure 3. This heatmap illustrates the correlation coefficients between various pairs of collimator rotation angle and selected clinical variables.

Figure 3 illustrates the correlation analysis between various collimator rotation pairs and multiple variables in patient treatment plans. Notably, the MCS, γ-index values, and HI values exhibited higher correlations among these variables. Specifically, the MCS showed a notably positive correlation with certain CRAs, like 30°/30° and 45°/45°. The γ-index value, indicative of dose delivery accuracy, was more strongly correlated with 2-arcs than 4-arcs, demonstrating an enhanced association with lower angles, particularly at 15°/15°. Similarly, the Homogeneity Index, essential for uniform dose distribution within the target volume, displayed a higher correlation with 2-arcs and favored lower angles such as 15°/15°.

Contrastingly, the dose variables related to the bladder and rectum did not exhibit a consistent correlation pattern, suggesting that the protection of risk organs like the bladder and rectum is less impacted by variations in collimator rotation angles.

Figure 4. Machine learning analysis of variable impact on CRAs. (a) Presents the Mean Relative Error for different CRAs, showcasing the variability in the model's predictive accuracy with respect to different collimator rotation pairs. (b) Demonstrates the Feature Importances from a Random Forest algorithm, revealing the relative impact of various planning variables on the CRAs' predictions.

Figure 4(a) presents the percentages of mean relative error for various CRAs in the context of radiotherapy. These figures represent the accuracy of the predictive model, indicating how closely the model's predictions matched the actual clinical data. The lowest mean relative error is observed for the 15°/0° at 10.43%, indicating that the model's predictions were closest to the actual values for this collimator angle. This could represent a more consistent or predictable pattern of treatment outcomes at this angle. Conversely, the highest mean relative errors are observed for the 15°/285° and 45°/315° at 12.72% and 12.58%, respectively. The remaining CRAs exhibit mean relative errors ranging from 11.06–11.91%, indicating that specific angles do not significantly impact the performance of the model.

Figure 4(b) illustrates the feature importances derived from a Random Forest model. The MCS stands out with the highest importance, approximately 0.19, suggesting its predominant impact on the model's predictions. Following MCS, the γ- index shows significant importance at 0.07. Various dose levels received by the bladder and rectum (D15%, D25%, D35%, D50%), along with the mean doses to the bladder, rectum, and small bowel, exhibit importance values from 0.01 to 0.05. These values indicate the comparative influence of each feature within the model, with a higher value denoting greater contribution to the model's predictive capabilities.

4. DISCUSSION

This study aimed to investigate the impact of CRA in HVMAT on dose distribution to tumors and normal organs in prostate cancer patients. Given the rising interest in HVMAT for whole pelvic radiotherapy, assessing the beam delivery elements is vital yet remains limited in scope.

Our study confirmed that all angle-generated treatment plans met the average V95% target for the prescribed dose in the PTV. We used experimental approaches with 2-arcs and 4-arcs methods across

various CRA settings. Despite the irregular and non-standardized structures of PTV, bladder, and rectal volumes, the CRA choices demonstrated no significant differences in these volumes (Table 2, $p > 0.05$).

Within the study's parameters, the selected CRA angles did not significantly affect the conformity and homogeneity of radiation distribution to the target volume, as supported by non-significant differences ($p > 0.05$) in Table 2. This contrasts with Sun et al.'s VMAT study, where significant dosimetric improvements, including in the CI and HI, were observed as the collimator intersection angle ($\Delta\theta$) approached 90°, emphasizing the need for precise CRA optimization in VMAT [11].

In Table 3, the analysis of average MU and MCS values revealed some differences in treatment plan outcomes related to CRA choices. For instance, 2-arcs required fewer MUs, with an average range from 1190.1 to 1226.7, compared to 4-arcs, which at specific angles like 45°/315° indicated a higher MU value of 1337.4. However, these differences were not statistically significant ($p > 0.05$). The heatmap analysis of Pearson's correlation coefficient in Fig. 3 indicated stronger correlations for MCS, HI, and the γ-index at specific CRAs. Although these results suggest sensitivity to CRA settings for certain measurements, they do not provide a clear conclusion regarding CRA dependence.

The machine learning analysis (Fig. 4) revealed that the MRE between 2-arcs and 4-arcs configurations varied within 2%, indicating consistent predictive accuracy across different CRA settings. Notably, the impact of CRA on MCS emerged as significant in feature importance analysis, aligning with the MCS findings in Table 3 but not reaching statistical significance ($p > 0.05$). The study's key findings revealed that, unlike previous literature on VMAT, statistical and machine learning analysis in HVMAT did not show high correlations between CRA conditions and various variables, as evidenced by p-values exceeding 0.05. Even with four arcs in HVMAT, the intersection of collimator angles had minimal impact on dose reduction in critical organs, suggesting that angle dependency in VMAT may not translate to HVMAT. Overall, this study suggests that machine learning analysis can reveal distinctions not readily apparent in traditional statistical methods. The Random Forest model emphasized the significance of certain features, like the MCS, in predicting treatment outcomes. These machine learning findings, combined with traditional statistical analysis, underscore the multidimensional nature of treatment plan optimization in HVMAT. This comprehensive approach is pivotal in better understanding the subtle impacts of CRA settings and plays a crucial role in advancing the clinical application of HVMAT, particularly in optimizing treatment plans and enhancing delivery efficiency.

However, it is essential to consider several limitations. First, the limited sample size and demographic diversity of the patient cohort might affect the generalizability of the study's findings. Second, as the focus was specifically on prostate cancer, direct application of these results to treatments for other types of cancer may be challenging. Third, constraints associated with the utilized machine learning model, such as the type of algorithm or included features, could impact the robustness of the findings. Finally, the statistical power of the study is influenced by the size of the sample and the magnitude of observed effects, potentially limiting the ability to detect small yet clinically significant differences across various CRA settings.

5. CONCLUSIONS

In conclusion, our study demonstrates that in HVMAT for prostate cancer, different CRA settings, including both 2-arcs and 4-arcs, do not substantially affect dose distribution to the target and normal organs. This suggests that CRA selection can be flexible without affecting treatment effectiveness. Additionally, our research highlights the complementary role of machine learning in analyzing complex treatment variables alongside conventional statistical methods, enhancing our understanding and interpretations. Despite the study's limitation due to the lack of individualized adjustments in treatment planning, our findings provide significant contributions to the field of HVMAT, potentially influencing future clinical practices and enhancing patient care.

Abbreviations

VMAT: Volume-modulated arc therapy

PTV: Planning target volumes

MLC: Multi-leaf collimator

OAR: Organ at risks

CRA: Collimator rotation angle

HVMAT: Half-Volume modulated arc therapy

CAX: Central axis

CI: Conformity index

HI: Homogeneity index

CT: Computed tomography

CTV: Clinical target volume

RTOG: Radiation Therapy Oncology Group

CW: Clockwise

CCW: Counterclockwise

DVH: Dose-volume histogram

CN: Conformation number

NTCP: Normal tissue complication probability

LKB: Lyman-Kutcher-Burman

EUD: Equivalent uniform dose

MCS: Modulation complexity score

γ-index: Gamma index

LINAC: Linear accelerator

LSV: Leaf sequence variability

AAV: Aperture area variability

QA: Quality assurance

MRE: Mean relative error

MU: Monitor unit

Declarations

Availability of data materials

Research data are stored in an institutional repository and will be shared upon request to the corresponding author.

Author information

Authors and Affiliations

Department of Radiation Oncology, Keimyung University Dongsan Hospital, Keimyung University School of Medicine, Dae-gu, 1035, Korea (South)

Myeongsoo Kim, Byungyong Kim, Euncheol Choi , Yun Sung Shin, Seung Gyu Park, Young Kee Oh, Sang Jun Byun

Contributions

M.K. and B.K. composed the manuscript, focusing on drafting and refining the content. SJ.B. contributed to the manuscript, ensuring accuracy in the content. YS.S. developed all treatment plans, aligning them with the study's aims. M.K. and E.C. analyzed data and produced the graphical representations in the study. Finally, SG.P and YK.O reviewed the final manuscript to ensure its academic quality and integrity.

Corresponding author

Correspondence to Sang Jun Byun

Ethics declarations

Ethical approval

This research was conducted in accordance with institutional guidelines and the Declaration of Helsinki of 1975 in its latest version. Ethical approval was granted by the ethics committee of Keimyung University Dongsan Hospital on February 10th, including a waiver of written informed consent, and to ensure patient privacy, all data was anonymized (IRB file No. 2023-02-019).

Consent for publication

Not applicable.

Competing interests

Not applicable.

Conflicts of interest

No conflicts of interest

References

1. Teoh M, Clark CH, Wood K, Whitaker S, Nisbet A. Volumetric modulated arc therapy: a review of current literature and clinical use in practice. British Journal of Radiology. 2011;84(1007):967-96.
2. Yu CX, Tang G. Intensity-modulated arc therapy: principles, technologies and clinical implementation. Phys Med Biol. 2011;56(5):R31-54.
3. Unkelbach J, Bortfeld T, Craft D, Alber M, Bangert M, Bokrantz R, et al. Optimization approaches to volumetric modulated arc therapy planning. Medical Physics. 2015;42(3):1367-77.
4. Giorgia N, Antonella F, Eugenio V, Alessandro C, Filippo A, Luca C. What is an acceptably smoothed fluence? Dosimetric and delivery considerations for dynamic sliding window IMRT. Radiation Oncology. 2007;2(1):42.
5. MMohan R, Arnfield M, Tong S, Wu Q, Siebers J. The impact of fluctuations in intensity patterns on the number of monitor units and the quality and accuracy of intensity modulated radiotherapy.

Medical Physics. 2000;27(6):1226-37.

6. Li C, Tao C, Bai T, Li Z, Tong Y, Zhu J, et al. Beam complexity and monitor unit efficiency comparison in two different volumetric modulated arc therapy delivery systems using automated planning. BMC Cancer. 2021;21(1):261.

7. Bai S, Li G, Wang M, Jiang Q, Zhang Y, Wei Y. Effect of MLC leaf position, collimator rotation angle, and gantry rotation angle errors on intensity-modulated radiotherapy plans for nasopharyngeal carcinoma. Med Dosim. 2013;38(2):143-7.

8. Kim J-i, Ahn BS, Choi CH, Park JM, Park S-Y. Optimal collimator rotation based on the outline of multiple brain targets in VMAT. Radiation Oncology. 2018;13(1):88.

9. Li M-H, Huang S-F, Chang C-C, Lin J-C, Tsai J-T. Variations in dosimetric distribution and plan complexity with collimator angles in hypofractionated volumetric arc radiotherapy for treating prostate cancer. Journal of Applied Clinical Medical Physics. 2018;19(2):93-102.

10. Sandrini ES, da Silva AX, da Silva CM. Evaluation of collimator rotation for volumetric modulated arc therapy lung stereotactic body radiation therapy using flattening filter free. Applied Radiation and Isotopes. 2018;141:257-60.

11. S Sun W, Chen K, Li Y, Xia W, Dong L, Shi Y, et al. Optimization of collimator angles in dual-arc volumetric modulated arc therapy planning for whole-brain radiotherapy with hippocampus and inner ear sparing. Sci Rep. 2021;11(1):19035.

12. Tas B, Bilge H, Ozturk ST. An investigation of the dose distribution effect related with collimator angle in volumetric arc therapy of prostate cancer. J Med Phys. 2016;41(2):100-5.

13. Lyu Q, O'Connor D, Ruan D, Yu V, Nguyen D, Sheng K. VMAT optimization with dynamic collimator rotation. Medical Physics. 2018;45(6):2399-410.

14. Hajdok G. Large, Half-Beam, Flattening Filter-Free Volumetric Modulated Arc Therapy for Head and Neck Cancer Radiation Therapy. International Journal of Radiation Oncology, Biology, Physics. 2014;90(1):S944.

15. Keil J, Carda J, Reihart J, Seidel M, Lenards N, Hunzeker A. A dosimetric study using split x-jaw planning technique for the treatment of endometrial carcinoma. Med Dosim. 2020;45(3):278-83.

16. Jang H, Park J, Artz M, Zhang Y, Ricci JC, Huh S, et al. Effective Organs-at-Risk Dose Sparing in Volumetric Modulated Arc Therapy Using a Half-Beam Technique in Whole Pelvic Irradiation. Frontiers in Oncology. 2021;11.

17. Yu P-C, Wu C-J, Nien H-H, Lui LT, Shaw S, Tsai Y-L. Half-beam volumetric-modulated arc therapy in adjuvant radiotherapy for gynecological cancers. Journal of Applied Clinical Medical Physics. 2022;23(1):e13472.

18. Small W, Jr., Bosch WR, Harkenrider MM, Strauss JB, Abu-Rustum N, Albuquerque KV, et al. NRG Oncology/RTOG Consensus Guidelines for Delineation of Clinical Target Volume for Intensity Modulated Pelvic Radiation Therapy in Postoperative Treatment of Endometrial and Cervical Cancer: An Update. Int J Radiat Oncol Biol Phys. 2021;109(2):413-24.

19. Chiavassa S, Bessieres I, Edouard M, Mathot M, Moignier A. Complexity metrics for IMRT and VMAT plans: a review of current literature and applications. British Journal of Radiology. 2019;92(1102).

20. Cao T, Dai Z, Ding Z, Li W, Quan H. Analysis of different evaluation indexes for prostate stereotactic body radiation therapy plans: conformity index, homogeneity index and gradient index. Precision Radiation Oncology. 2019;3(3):72-9.

21. van't Riet A, Mak AC, Moerland MA, Elders LH, van der Zee W. A conformation number to quantify the degree of conformality in brachytherapy and external beam irradiation: application to the prostate. Int J Radiat Oncol Biol Phys. 1997;37(3):731-6.

22. Luxton G, Keall PJ, King CR. A new formula for normal tissue complication probability (NTCP) as a function of equivalent uniform dose (EUD). Phys Med Biol. 2008;53(1):23-36.

23. McNiven AL, Sharpe MB, Purdie TG. A new metric for assessing IMRT modulation complexity and plan deliverability. Med Phys. 2010;37(2):505-15.

24. Lam D, Zhang X, Li H, Deshan Y, Schott B, Zhao T, et al. Predicting gamma passing rates for portal dosimetry-based IMRT QA using machine learning. Medical Physics. 2019;46(10):4666-75.

25. Fiandra C, Cattani F, Leonardi MC, Comi S, Zara S, Rossi L, Jereczek-Fossa BA, Fariselli P, Ricardi U, Heijmen B. Machine Learning for Predicting Clinician Evaluation of Treatment Plans for Left-Sided Whole Breast Radiation Therapy. Adv Radiat Oncol. 2023 Apr 29;8(5):101228. doi: 10.1016/j.adro.2023.101228. PMID: 37405256; PMCID: PMC10316432.

26. Smith WP, Kim M, Holdsworth C, Liao J, Phillips MH. Personalized treatment planning with a model of radiation therapy outcomes for use in multiobjective optimization of IMRT plans for prostate cancer. Radiation Oncology. 2016;11(1):38.

Tables

Tables are available in the Supplementary Files section.
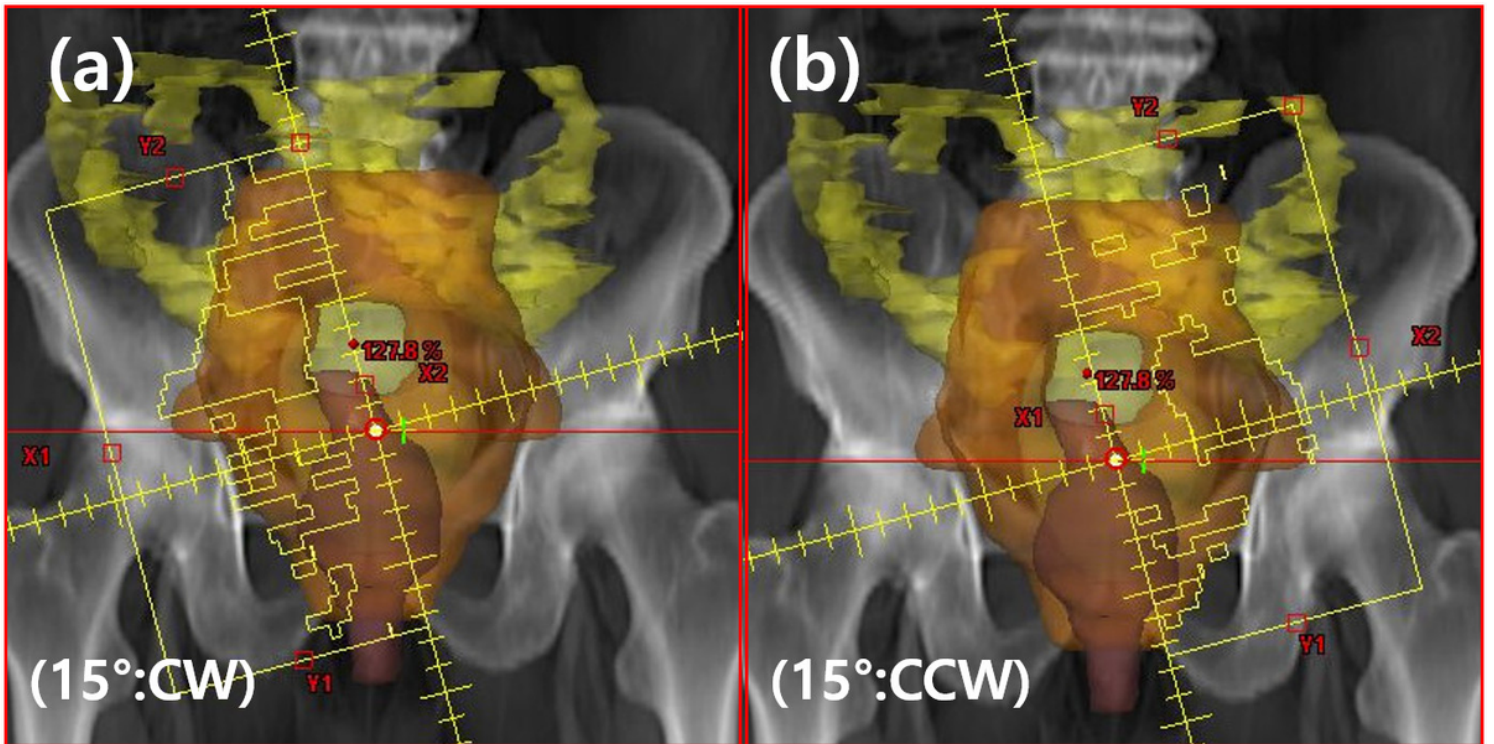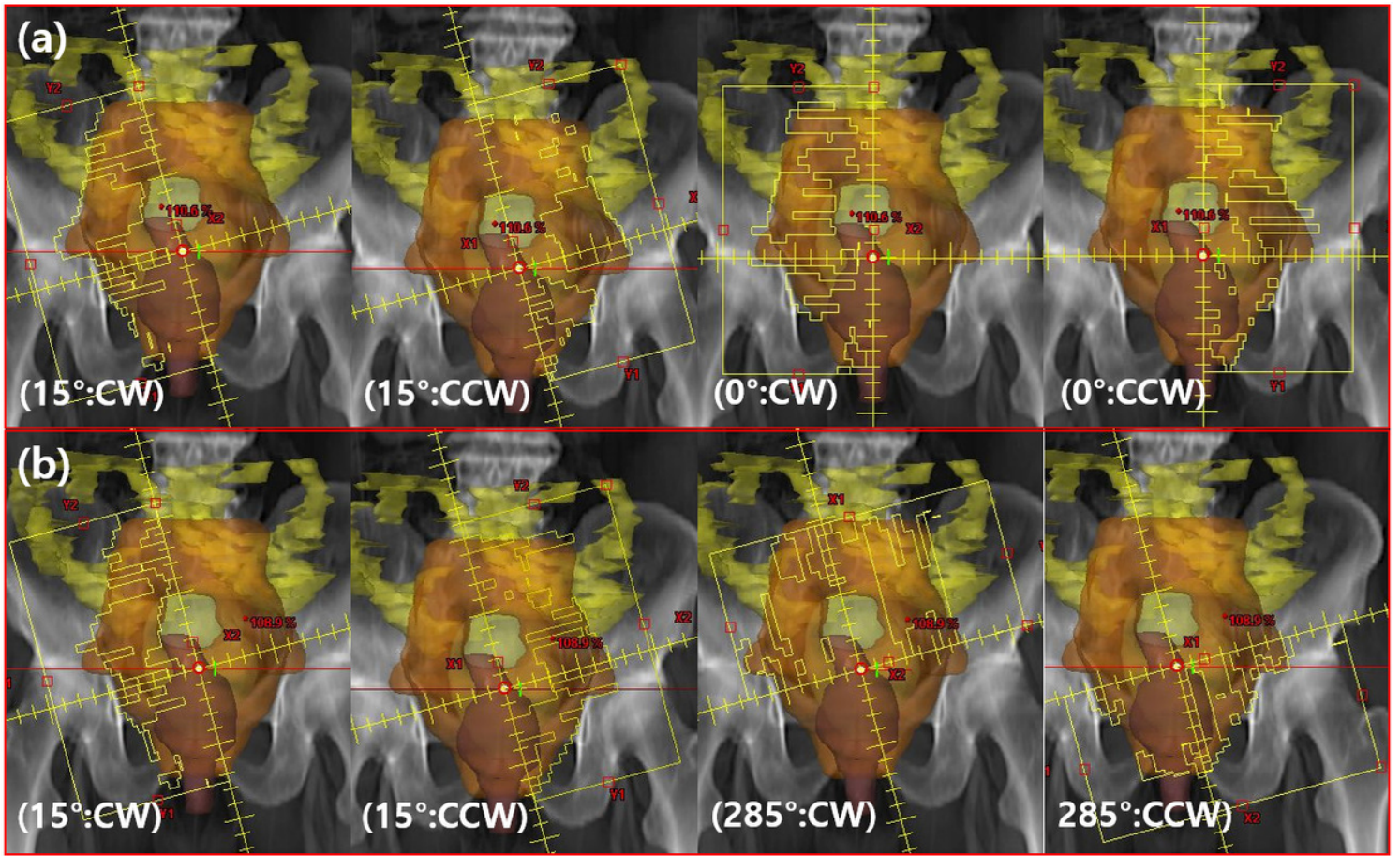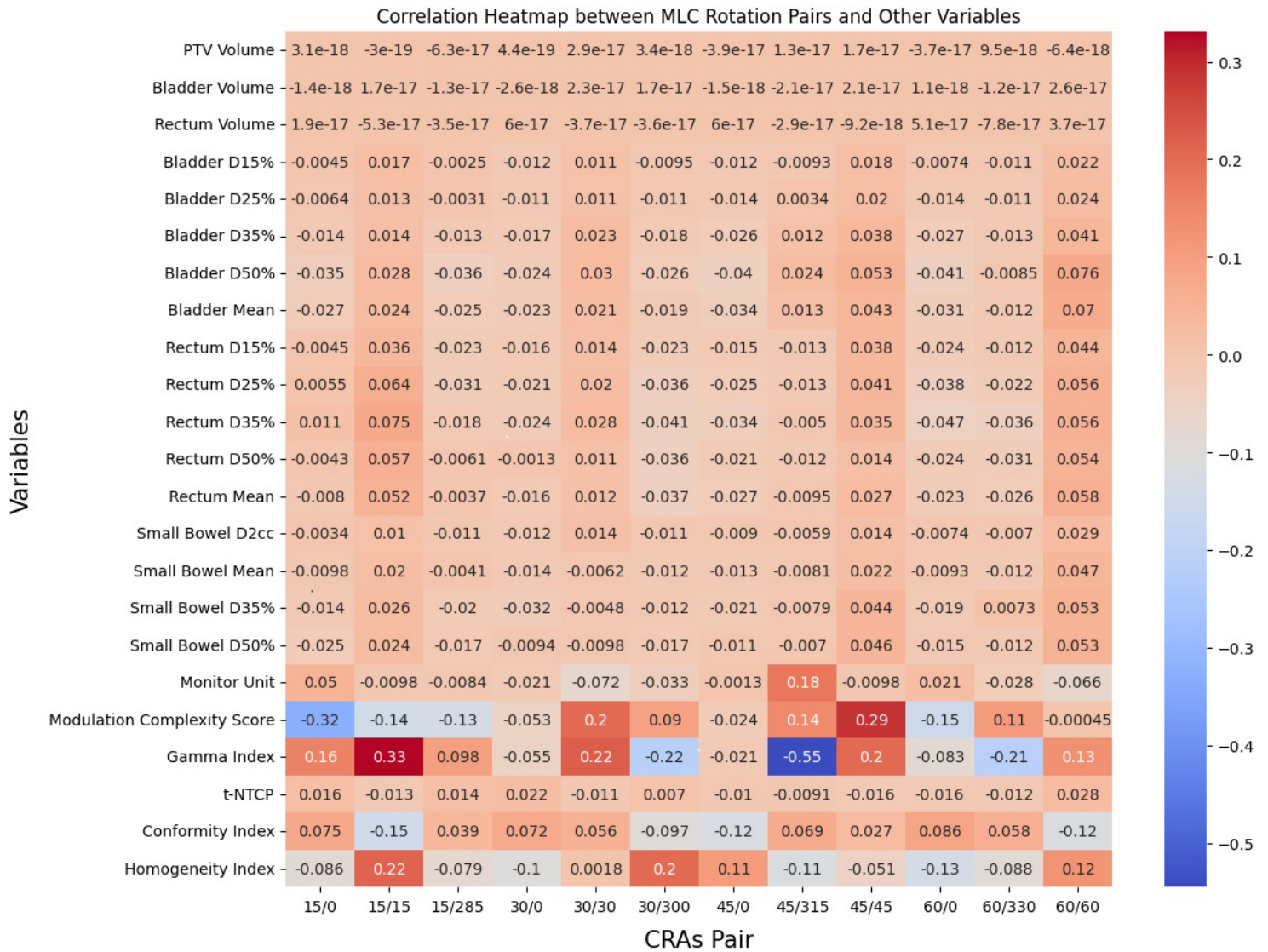
Figures

Figure 1

Patient #5, Example of collimator rotation angle 15°/15°: Beam's eye view of half-beam volumetric modulated arc therapy including the half-beam fields corresponding to 2-arcs of gantry rotation: (a) counterclockwise (Gantry rotation angle: 179.0°−181.0°) and (b) clockwise (Gantry rotation angle: 181.0°−179.0°).
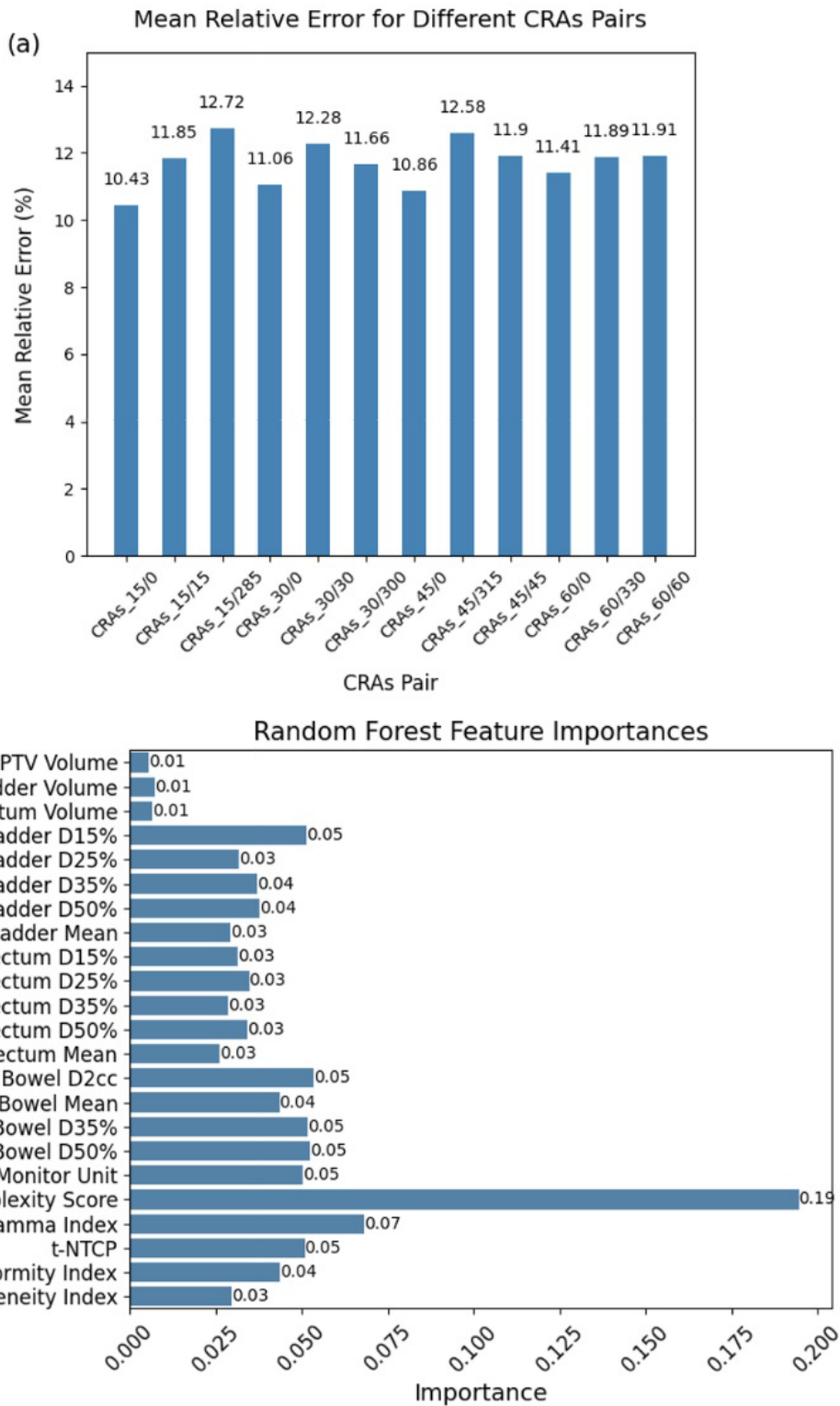
Figure 2

Patient #5, Example of collimator rotation angles 15°/0° and 15°/285°: Beam's eye view of half-beam volumetric modulated arc therapy, encompassing the half-beam fields corresponding to 4-arcs of gantry rotation: (a) 4-arcs with collimator rotation angle 15°/0°, and (b) 4-arcs with collimator rotation angle 15°/285°.

Figure 3

This heatmap illustrates the correlation coefficients between various pairs of collimator rotation angle and selected clinical variables.

Figure 4

Machine learning analysis of variable impact on CRAs. (a) Presents the Mean Relative Error for different CRAs, showcasing the variability in the model's predictive accuracy with respect to different collimator rotation pairs. (b) Demonstrates the Feature Importances from a Random Forest algorithm, revealing the relative impact of various planning variables on the CRAs' predictions.

Supplementary Files

This is a list of supplementary files associated with this preprint. Click to download.

- Table1.jpg
- Table2.jpg
- Table3.jpg